

An Element-wise, Locally Conservative Galerkin (LCG) Method for Diffusion and Convection-Diffusion Problems.

P. Nithiarasu^{*} and C.G. Thomas

School of Engineering, University of Wales Swansea, Swansea SA2 8PP, UK

Abstract

An element-wise, Locally Conservative Galerkin (LCG) method is employed to solve the conservation equations of diffusion and convection-diffusion. This approach allows the system of simultaneous equations to be solved over each element. Thus, the traditional assembly of elemental contributions into a global matrix system is avoided. This simplifies the calculation procedure over the standard continuous Galerkin method, in addition to explicitly establishing element-wise flux conservation. The elements are treated as sub-domains with a weakly imposed Neumann boundary condition. The LCG method obtains a continuous and unique nodal solution from the surrounding element contributions via averaging. It is also shown in this paper that the proposed LCG method is identical to the standard Global Galerkin (GG) method, at both steady and unsteady states, for an inside node. Thus, the method has all the advantages of the standard GG method while explicitly conserving fluxes over each element.

Several problems of diffusion and convection-diffusion are solved on both structured and unstructured grids to demonstrate the accuracy and robustness of the LCG method. Both linear and quadratic elements are used in the calculations.

Key words: explicit local flux conservation, element-by-element solution, heat conduction, convection-diffusion, Characteristic-Galerkin (CG), SUPG, linear and quadratic finite elements

^{*} Correspondence to Dr P. Nithiarasu

Email addresses: P.Nithiarasu@swansea.ac.uk, cgthomas@swansea.ac.uk (C.G. Thomas).

1 Introduction

Local conservation is a desirable property in numerical modelling of engineering problems. Finite volume methods are known to conserve fluxes in a given dual cell around a node. The finite element form for an equation of the type $\partial F_i/\partial x_i$, may be written for a sub-domain surrounding a node as

$$\int_{\Omega} -\frac{\partial w^a}{\partial x_i} \tilde{F}_i d\Omega + \int_{\Gamma} w^a \tilde{F}_i d\Gamma = 0 \quad (1)$$

For the Galerkin approximation, the sum of the derivatives of the weight function surrounding an inside node a is zero and thus the flux is conserved. An argument similar to the one in Equation 1 can also be used for an inside element. However, the standard finite element formulation is carried out by canceling the opposing fluxes on the inside edges, resulting in a globally conservative form if the boundaries are Neumann type [1–6]. Though such standard procedure implicitly conserves local fluxes, explicit conservation of local fluxes is only obvious if the flux terms at the element edges are retained.

Recently, the Discontinuous Galerkin Method (DGM) has received a great deal of attention [7–19]. A decent overview of the topic is given by Cockburn, Karniadakis and Shu [17]. Despite favourable properties such as local conservation, natural extension of the method to any order approximation and discontinuity capturing at domain interfaces, DGM method is more expensive than continuous or global Galerkin method. The excessive number of freedoms and the higher cost associated with it are often blamed for DGM’s lack of interest within the engineering industry. Thus, it is not surprising researchers are looking for a DGM with a structure of continuous Galerkin method [20]. However, we believe that it would be easier to modify a continuous Galerkin structure to adopt a discontinuous path [21] rather than adopting DGM to develop a global Galerkin structure. This way, existing industrial codes can be modified to accommodate the changes without resorting to complete revision of the codes. The proposed element-by-element approach, in theory, is identical to the standard Galerkin method apart from the global boundaries and easy to implement. At global boundaries, an extra Neumann condition is applied to make the method explicitly conserve fluxes both locally and globally. Such a procedure allows the elements to be treated as individual sub-domains.

Though the work of Hughes and co-workers [5,6] rekindled the conservation issue of the finite element methods, element-by-element solution of the conservation equations, using a standard Galerkin structure is not addressed. Our previous work proved that the element-by-element solution is possible via postprocessing the fluxes at every time step [21]. This flux is then weakly imposed on element boundaries and this allowed the computational domain

to be broken down into a series of elemental sub-domains. Though reasonable accuracy was achieved previously, the approximations used for postprocessing did not allow a direct comparison with the global Galerkin (GG) method. In the present paper, we have adopted a more standard form for linear elements to prove that the LCG method is identical to the GG method for an inside node. In addition to providing results using linear elements, we also have extended the study to quadratic elements. We have also discussed some better ways of postprocessing the fluxes for quadratic elements.

The paper is organised into following sections. We define the problem in the following section. We describe the LCG method and compare it to the global Galerkin method in Section 3. The implemented approach is thoroughly tested on steady state heat conduction and scalar convection-diffusion in Section 4 using quadratic elements. Influences of various factors such as source terms, mesh variations and time discretization are also investigated in Section 4. Finally, Section 5 draws some conclusions.

2 Problem Statement

The conservation statement of a scalar variable, ϕ , may be written as

$$\beta \frac{\partial \phi}{\partial t} + \frac{\partial F_i}{\partial x_i} + Q = 0 \quad (2)$$

where β is a constant, F_i are the flux components in the directions x_i of a Cartesian co-ordinate system and Q is a source term. Generally F_i consists of both convective and diffusive flux components, but it can also be purely diffusive or convective. The solution of this equation is sought over Ω . To complete the problem, information on initial and boundary conditions is also required and is taken to be given in the form

$$\begin{aligned} \phi(\mathbf{x}, t = 0) &= \phi_0(\mathbf{x}) \quad \forall \mathbf{x} \in \Omega \\ \phi &= \bar{\phi}(\mathbf{x}, t) \quad \text{on } \Gamma_\phi \quad \text{and} \\ F_n &= \bar{F}(\mathbf{x}, t) \quad \text{on } \Gamma_f \end{aligned} \quad (3)$$

Here the domain boundary, Γ , of Ω is decomposed as

$$\Gamma = \Gamma_\phi \cup \Gamma_f \quad (4)$$

where Γ_ϕ and Γ_f represents the Dirichlet and Neumann partitions.

3 Global Galerkin and Locally Conservative Galerkin (LCG) Forms

3.1 Global Galerkin (GG) Discretization

The variation of the scalar variable over an n -node element is approximated as

$$\phi \approx \tilde{\phi} = \sum_{a=1}^n N_a \phi_a = \mathbf{N}\Phi \quad (5)$$

where $\tilde{\phi}$ is an approximation of the scalar quantity and subscript a indicates nodes. Using the method of weighted residuals, Equation (2) is written as (source term is neglected for simplicity)

$$\beta \int_{\Omega} w_a \frac{\Delta \tilde{\phi}}{\Delta t} d\Omega = - \int_{\Omega} w_a \frac{\partial \tilde{F}_i^n}{\partial x_i} d\Omega \quad (6)$$

where $w_a(\mathbf{x})$ are the arbitrary weighting functions. Performing integration by parts to the RHS term of Equation (6) gives

$$\beta \int_{\Omega} w_a \frac{\Delta \tilde{\phi}}{\Delta t} d\Omega = \int_{\Omega} \frac{\partial w_a}{\partial x_i} \tilde{F}_i^n d\Omega - \int_{\Gamma} w_a \tilde{F}_i^n d\Gamma n_i \quad (7)$$

where n_i are the components of the outward normal vector to the boundary.

3.2 Locally Conservative Galerkin (LCG) Discretization

In the LCG method the variable and its fluxes are explicitly conserved over each individual element. This is achieved through the calculation of a numerical flux at element boundaries. This also ensures that continuity between neighboring elements is maintained. Such a process is equivalent to treating the global domain as a group of elemental sub-domains; each with its own set of time-dependent Neumann boundary conditions prescribed at each time step. With a numerical flux being available at the element edges, Equation (7) is rewritten in the LCG form for solving over an elemental subdomain Ω_e as

$$\beta \int_{\Omega_e} \mathbf{N}^T \mathbf{N} \frac{\Delta \Phi}{\Delta t} d\Omega_e = \int_{\Omega_e} \frac{\partial \mathbf{N}^T}{\partial x_i} \tilde{F}_i^n d\Omega_e - \int_{\Gamma_e} \mathbf{N}^T \hat{\tilde{F}}_i^n d\Gamma_e n_i \quad (8)$$

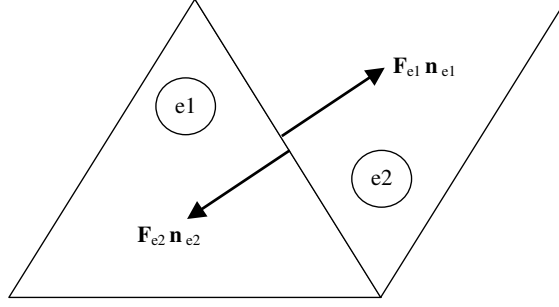


Fig. 1. Flux crossing a common edge between two elements

The boundary integral term of Equation (8) is approximated with a computed value of flux, \hat{F}_i , across the element edges.

The flux boundary condition at the element edges is weakly enforced by making it equal and opposite as shown in Figure 1. A post-calculation is made at the end of each time-step to obtain the interface fluxes on each of the element edges. Using the computed edge flux on the element boundaries of adjoining elements, the following condition is enforced:

$$\mathbf{F}_{e1} \mathbf{n}_{e1} = \mathbf{F}_{e2} \mathbf{n}_{e2} \quad (9)$$

The subscripts are defined in Figure 1. Some procedures for estimating this flux is described later. The matrix form of Equation (8) is written as

$$\beta[\mathbf{M}_e]\{\Delta\Phi\} = \Delta t([\mathbf{K}_e]\{\Phi\}^n + \{\mathbf{f}_{r_e}\}^n) \quad (10)$$

and the system of simultaneous equations are solved over individual elements independently of surrounding element equation sets. An implicit solution procedure is also possible and is obtained by treating part of the flux term implicitly to give

$$[\beta\mathbf{M}_e + \Delta t\mathbf{K}_e]\{\Phi\}^{n+1} = [\mathbf{M}_e]\{\Phi\}^n + \Delta t\{\mathbf{f}_{r_e}\}^n \quad (11)$$

In both the explicit and implicit form (given by Equations (10) and (11)), the mass matrix, \mathbf{M}_e , may either be lumped, or kept as a consistent mass matrix. For simple linear-triangular elements \mathbf{M}_e can be lumped by summing-up the rows. Lumping quadratic-triangular elements in this way gives zero diagonal terms. An alternative is shown in Figure 2 [22], which is used in this paper. This procedure treats one quadratic element as 4 linear elements for lumping the mass matrix.

A situation of multiple solutions being calculated at global mesh nodes is eliminated by taking an arithmetic mean of nodal values obtained from different

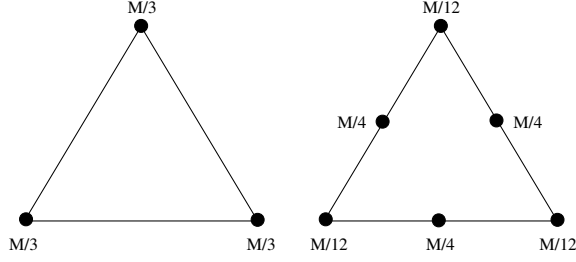


Fig. 2. Lumping parameters for linear and quadratic triangles

elemental contributions to a node. This is necessary as it provides a unique solution throughout the domain.

3.3 LCG Methods for Convection Dominated Flows

To overcome difficulties at elevated values of Péclet numbers, suitable discretization of the convection-diffusion equation is needed. Standard methods such as Streamline Petrov-Galerkin (SUPG) and Characteristic Galerkin (CG) can readily be employed using LCG discretization. The extra stabilizing or higher order terms resulting from the discretization are treated explicitly and locally. For the SUPG method, special weighting for transient terms is not used. In addition, the third and higher order terms are neglected.

3.3.1 SUPG Method

The following weighting function is used For SUPG stabilization [23]

$$w_a = N_a + \frac{\alpha h}{2} \frac{U_i}{|\mathbf{U}|} \frac{\partial N_a}{\partial x_i} \quad (12)$$

where, for linear triangles the optimal value of α is given by

$$\alpha = \alpha_{opt} = \coth(Pe) - \frac{1}{(Pe)} \quad (13)$$

and the element Péclet number, Pe , is calculated from

$$Pe = \frac{|\mathbf{U}|h}{2k} \quad (14)$$

here h is the element size, there are a number of ways of calculating element size. For a known, unchanging velocity field, the element size can be computed

in the streamline direction [23,24], and will only need to be performed once at the pre-processing stage.

Application of the optimal stabilizing parameters for quadratic triangular elements follows the application of the SUPG method for one-dimensional quadratic elements [23,25]. It involves calculating separate stabilizing parameters for the centre and the end nodes. The optimal parameter for the mid-side node is the same as linear elements and is given by Equation (13). At the corner nodes the optimal value of α is given by

$$\alpha_{opt} = \frac{(2Pe - 1) + (-6Pe + 7)e^{-2Pe} + (-6Pe - 7)e^{-4Pe} + (2Pe + 1)e^{-6Pe}}{(Pe + 3) + (-7Pe - 3)e^{-2Pe} + (7Pe - 3)e^{-4Pe} - (Pe + 3)e^{-6Pe}} \quad (15)$$

3.3.2 CG Method

There are a number of variations of the CG method available. Here, we use the "simple explicit characteristic Galerkin procedure", as described by Löhner et al. [27] and Zienkiewicz et al. [26]. It has been the basis of the characteristic-based-split (CBS) algorithm [28–30]. Temporal discretization of Equation (2), using the simple characteristic based procedure gives

$$\beta \frac{\phi^{n+1} - \phi^n}{\Delta t} = -\frac{\partial F_i^n}{\partial x_i} - Q + \frac{\Delta t}{2} u_k \frac{\partial}{\partial x_k} \left(\frac{\partial F_i}{\partial x_i} + Q \right)^n + O(\Delta t^2) \quad (16)$$

In this form the Galerkin weighting

$$w_a = N_a \quad (17)$$

is optimal and will produce non-oscillatory results, subject to stability conditions. In this work the boundary contribution arising from integration by parts of the extra second-order terms in Equation (16) are neglected [26].

4 Comparison Between GG and LCG Methods

To carry out a direct comparison between the GG and LCG method, we consider the transient convection-diffusion equation in one dimension without the source term. In GG form, without stabilization, the assembled nodal equation for an inside node i (see Figure 3) using linear elements is given as (Equation 7)

$$\beta \left(\frac{h_1 + h_2}{2} \right) \frac{\Delta \phi_i}{\Delta t} = \frac{u}{2} (\phi_{i-1} - \phi_{i+1}) - \nu \left(\frac{\phi_{i-1}}{h_1} - \frac{\phi_i}{h_1} - \frac{\phi_i}{h_2} + \frac{\phi_{i+1}}{h_2} \right) \quad (18)$$

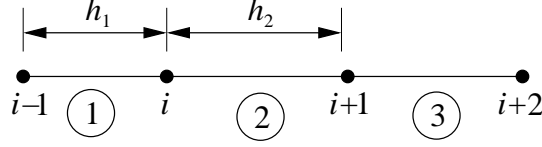


Fig. 3. A typical linear one dimensional element patch

where ν is the diffusion coefficient and u is the convection velocity. The mass matrix in the above equation is lumped to simplify presentation. In LCG form, we get two equations from the elements connected to the node i and we need Neumann conditions at the element boundaries (node i). The nodal values of the convection fluxes are calculated at the nodes. However, diffusion fluxes with second order derivatives are constant over the elements. The nodal value of such diffusion fluxes are determined by averaging the values over the surrounding elements. With such a post-processed flux, the equation for the node i from the first element may be written as (Equation 10)

$$\beta \frac{h_1}{2} \frac{\Delta \phi_i}{\Delta t} = \frac{u}{2} (\phi_{i+1} + \phi_i) + \frac{\nu}{h_1} (\phi_{i-1} - \phi_i) - u \phi_i + \frac{\nu}{2} \left[\frac{1}{h_1} (\phi_i - \phi_{i-1}) + \frac{1}{h_2} (\phi_{i+1} - \phi_i) \right] \quad (19)$$

The second line in the above equation represents the convection and diffusion fluxes at node i . Simplification gives

$$\beta \frac{h_1}{2} \frac{\Delta \phi_i}{\Delta t} = \frac{u}{2} (\phi_{i-1} - \phi_i) + \frac{\nu}{2h_1} (\phi_{i-1} - \phi_i) + \frac{\nu}{2h_2} (\phi_{i+1} - \phi_i) \quad (20)$$

Similarly the i th nodal equation from the second element is

$$\beta \frac{h_2}{2} \frac{\Delta \phi_i}{\Delta t} = \frac{u}{2} (\phi_i - \phi_{i+1}) + \frac{\nu}{2h_1} (\phi_{i-1} - \phi_i) + \frac{\nu}{2h_2} (\phi_{i+1} - \phi_i) \quad (21)$$

Sum of Equations (20) and (21) gives Eq. (18). This immediately shows that the GG and LCG methods are identical for an inside node. Same applies to quadratic elements. However, the diffusive fluxes, for quadratic elements, at the boundaries are calculated by averaging the two nodal values rather than elemental values.

To demonstrate the equivalence of the LCG and GG methods in two dimensions, consider a linear element patch as shown in Figure 4. The LCG nodal equation for node 1 from element 1 may, for the equation type (2) with only first derivatives with no source term, be written as

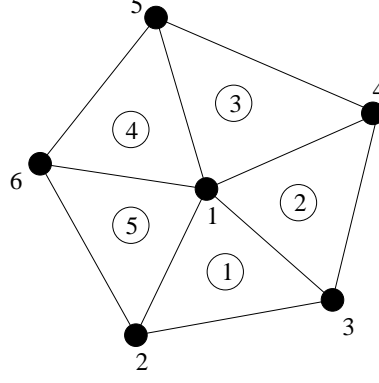


Fig. 4. A typical linear triangular element patch

$$\begin{aligned} \beta \frac{A_1}{3} \frac{\Delta \phi_1}{\Delta t} &= \frac{A_1}{3} b_1^1 (F_1^1 + F_1^2 + F_1^3) + \frac{A_1}{3} c_1^1 (F_2^1 + F_2^2 + F_2^3) \\ &\quad - \frac{x_2^2 - x_2^1}{6} (2F_1^1 + F_1^2) - \frac{x_2^1 - x_2^3}{6} (2F_1^1 + F_1^2) \\ &\quad - \frac{x_1^1 - x_1^2}{6} (2F_2^1 + F_2^2) - \frac{x_1^3 - x_1^1}{6} (2F_2^1 + F_2^2) \quad (22) \end{aligned}$$

Again a lumped mass matrix at LHS is assumed. The last four terms in the above equation represent the outward edge fluxes at the edges connected to the node 1 and b_1^1 and c_1^1 are the derivatives of the linear shape functions in x_1 and x_2 directions. The superscripts in the above equation represent the nodes and subscripts are used to indicate the directions and elements (in the case of A (area of the elements) and derivatives of shape functions). Substituting b_1^1 and c_1^1 values into Equation (22) and simplifying, we get

$$\begin{aligned} \beta \frac{A_1}{3} \frac{\Delta \phi_1}{\Delta t} &= F_1^1 (x_2^3 - x_2^2) + F_1^2 (x_2^1 - x_2^3) + F_1^3 (x_2^2 - x_2^1) \\ &\quad + F_2^1 (x_1^2 - x_1^3) + F_2^2 (x_1^3 - x_1^1) + F_2^3 (x_1^1 - x_1^2) \quad (23) \end{aligned}$$

Similarly four more equations from the four elements contributing to the node 1 can be derived. Adding all such equations results in

$$\begin{aligned} 2\beta(A_1 + A_2 + A_3 + A_4 + A_5) \frac{\Delta \phi}{\Delta t} &= \\ &F_1^2 (x_2^6 - x_2^3) + F_1^3 (x_2^1 - x_2^4) + F_1^4 (x_2^3 - x_2^5) + F_1^5 (x_2^4 - x_2^6) \\ &+ F_1^6 (x_2^5 - x_2^2) + F_2^2 (x_1^3 - x_1^6) + F_2^3 (x_1^4 - x_1^1) + F_2^4 (x_1^5 - x_1^3) \\ &\quad + F_2^5 (x_1^6 - x_1^4) + F_2^6 (x_1^2 - x_1^5) \quad (24) \end{aligned}$$

The above equation is identical to the one from an assembled GG method for an inside node. In a similar way the equivalence to the GG method can

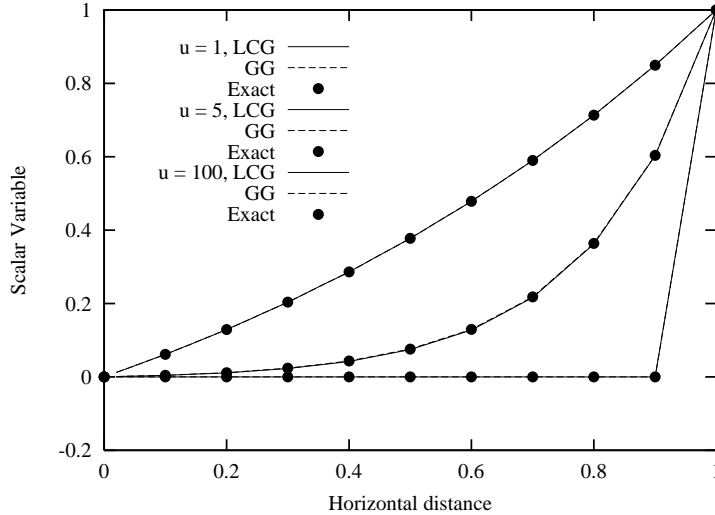


Fig. 5. One dimensional convection-diffusion problem. Scalar variable distribution for different convection velocities.

also be proved with second derivatives appearing in the equation. To further demonstrate the equivalence, three test problems of convection and convection diffusion are considered using linear elements. More robust tests are provided later with quadratic elements.

The first problem is the classical one dimensional problem with Dirichlet boundary conditions prescribed at both inlet and exit. A scalar variable value of zero was prescribed at the inlet and unity at exit. The variation of the scalar variable for different convection velocities are shown in Figure 5. Here, SUPG method was used with an optimal stabilization parameter. As seen the LCG, GG and exact solution are identical on a mesh with 10 elements.

The second problem considered is again a steady state problem but a more demanding problem in two dimension. It is a pure convection problem in a square domain with the scalar variable of zero prescribed along the bottom side. A small distance along the right vertical side from the bottom corner is also subjected to zero value of the scalar variable. The remaining length of the vertical side is subjected to a scalar variable value of unity. All other sides are natural boundaries. The velocity direction is skewed at 45° to the horizontal. A 39×39 structured, uniform mesh is used and the velocity direction is aligned with the mesh orientation. As seen from the Figure 6 that the solutions obtained from both LCG and CG are identical. The procedure used here is the CG method.

The third problem considered is the transient pure convection of a hill. This is one of the difficult problems and we are only interested in comparing the GG and LCG results for the same input values. The problem definition is as given by Donea et al. [31] and the results are shown in Figure 7. As seen, for

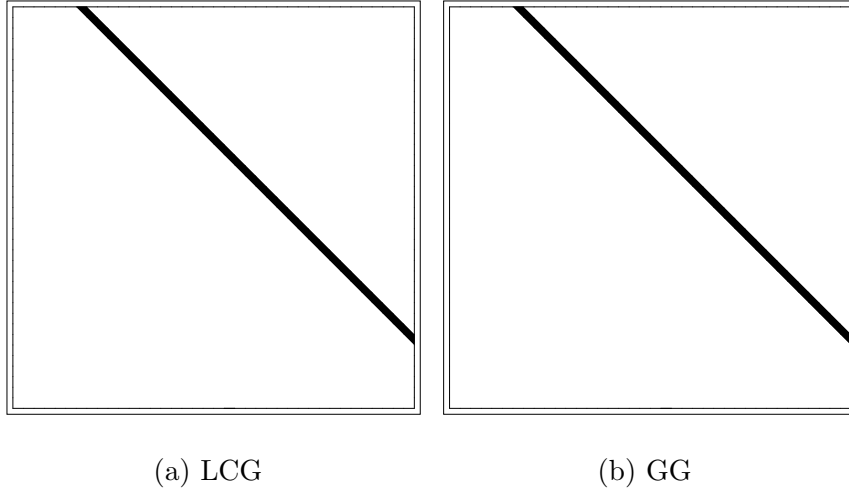


Fig. 6. A pure convection problem. Comparison between LCG and GG methods.

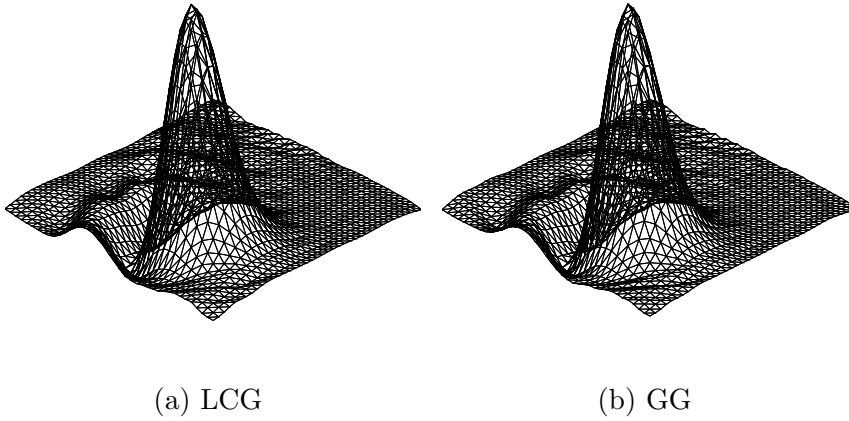


Fig. 7. A transient, pure convection problem. Comparison between LCG and GG methods.

the same number of time steps ($t = 2\pi$) and conditions, the results obtained are almost identical. The minor differences between the two results may be attributed to the extra boundary condition imposed by the LCG method at the global boundaries.

5 Edge Fluxes for Quadratic Elements

Figure 8 shows a number of quadratic elements connected to an arbitrary node a in Ω . The gradient $\frac{\partial \phi}{\partial x_i}$ at node a , is calculated by taking a mean average of the nodal gradient values from each element connected to this node. (marked

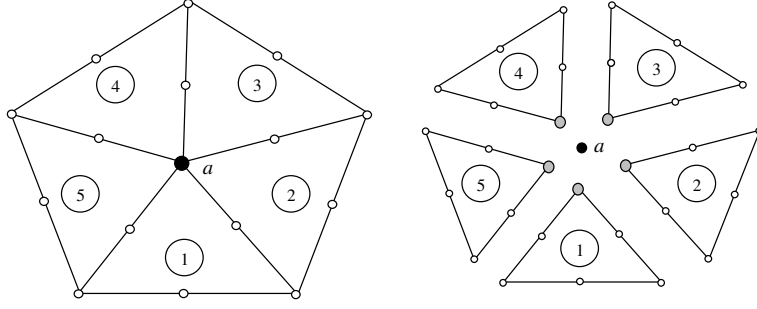


Fig. 8. A group of connecting elements sharing node a

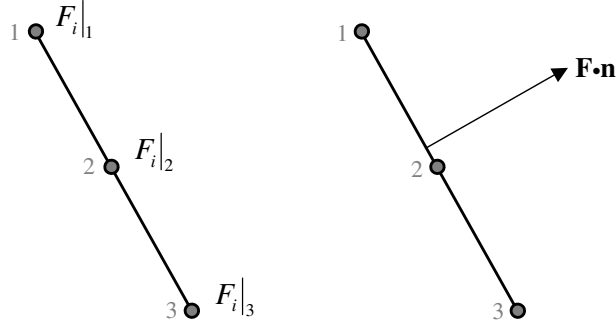


Fig. 9. Local edge node numbering for nodal fluxes, the final edge flux is formed from a weighted average of the nodal values.

grey in Figure 8), i.e;

$$\frac{\partial \phi}{\partial x_i} \Big|_a = \frac{1}{ne} \sum_{e=1}^{ne} \left\{ \frac{\partial \phi}{\partial x_i} \Big|_e \right\} \quad (25)$$

where ne is the total number of elements connected to a . In general the nodal fluxes, $F_i|_a$, will contain both a nodal diffusive flux component, and a nodal convective flux component, i.e.,

$$F_i|_a = F_i|_a \left(\frac{\partial \phi}{\partial x_i} \Big|_a, u_i \phi|_a \right) \quad (26)$$

Based on a lumped 1D quadratic element, the following weighted formula was used in the computation of the interface flux along an element edge (see Figure 9).

$$F_i = \frac{1}{6} (F_i|_1 + 4F_i|_2 + F_i|_3) \quad (27)$$

As mentioned earlier, this edge flux ensures continuity between elements.

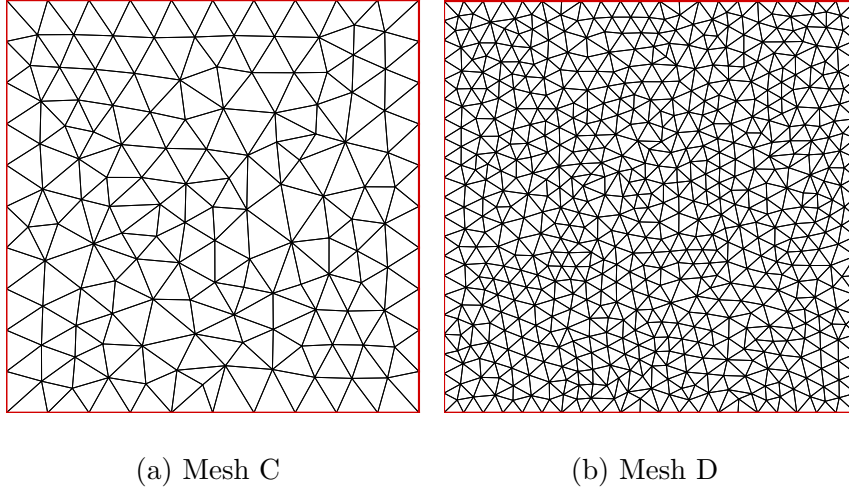


Fig. 10. Finite element meshes

6 More Examples Using Quadratic Elements

Three steady state examples are presented in this section. Since analytical solutions are available for some problems considered, robust testing of LCG method on quadratic elements is possible. Comparisons are also made against the GG results.

6.1 Finite Element Meshes

A number of structured and unstructured meshes have been employed in the proceeding sub-sections. Only unstructured meshes are shown in Figure 10. Mesh A is a coarse uniform structured mesh with 200 elements and Mesh B is a similar uniform structured grid, but a finer mesh with 800 elements (not shown). The last two meshes, Mesh C, and Mesh D, are unstructured grids with 266 and 1228 elements respectively.

6.2 Two Dimensional Steady State Heat Conduction

For heat conduction problems the flux is defined as

$$F_i = -k \frac{\partial T}{\partial x_i} \quad (28)$$

and the scalar variable ϕ in Equation (2) is replaced by the temperature T and coefficient β is replaced with ρc_p (heat capacity). The solution of steady-state

heat conduction is sought within a unit-square plate, subjected to Dirichlet boundary conditions on all its four sides. All the sides except the top side is subjected to a constant temperature of 100°C. The top side is subjected to 500°C.

The initial temperature of the plate was assumed to be at 0°C. A prescribed residual error tolerance of 1×10^{-09} was used to determine the steady state. The analytical solution for this problem is given by Holman [32] as

$$T = T_{side} + (T_{top} - T_{side}) \frac{2}{\pi} \sum_{n=1}^{\infty} \frac{(-1)^{n+1} + 1}{n} \sin\left(\frac{n\pi x_1}{w}\right) \frac{\sinh\left(\frac{n\pi x_2}{w}\right)}{\sinh\left(\frac{n\pi H}{w}\right)} \quad (29)$$

where w is the width, H is the height of the plate, T_{top} is the temperature at top side and T_{side} is the temperature at the other sides of the plate.

On each mesh, three different variations of the LCG method were tested. They are: LCG (explicit), LCG (implicit), and global Galerkin (explicit). In addition, for each of the three methods, consistent and lumped mass variations were also used. This produced six different solutions on each mesh. Results using structured Mesh A are shown in Figure 11 for both consistent and lumped mass versions. Very similar qualitative results were obtained on the other meshes.

As seen, all variations give rather smooth temperature contours. Generally the results are in close agreement with each other. However, closer inspection of the solutions given in Figure 11 shows that the consistent mass version of the global Galerkin method is the least accurate and is similar to the explicit LCG method with a consistent mass. The results obtained from consistent mass version of the Implicit LCG method are much better showing excellent symmetry with respect to mid-vertical line. The lumped mass versions of both the explicit and implicit LCG method and the lumped mass global Galerkin method are also highly symmetric.

The temperatures computed along the mid-horizontal and mid-vertical lines are compared against the exact solution in Figure 12. As seen the lumped mass explicit LCG method and the lumped mass explicit global Galerkin method, along with both lumped and consistent mass versions of the implicit LCG method, give excellent agreement with the exact solution. The explicit global Galerkin and LCG methods with consistent mass were found to be less accurate on both meshes. Table 1 gives the total CPU time taken by all six variations to converge to a prescribed steady state tolerance. The major advantage of using the consistent form of the explicit LCG method, instead of the global Galerkin version, is that the LHS mass matrix can be inverted by hand to save CPU costs. This is reflected in Table 1. As expected, both of the

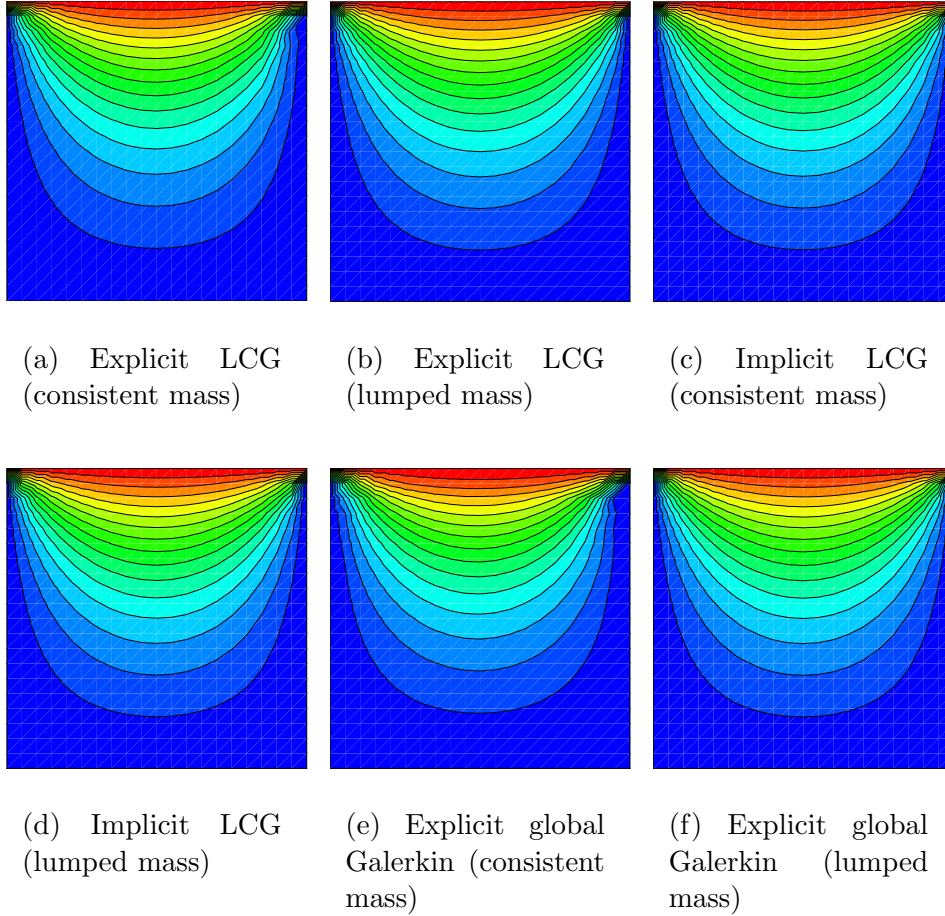
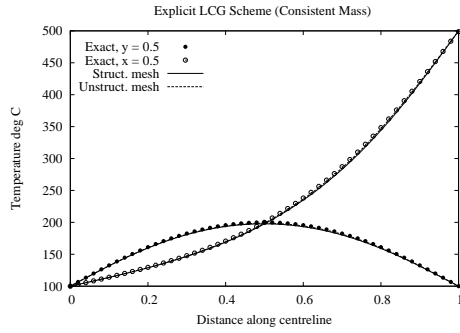


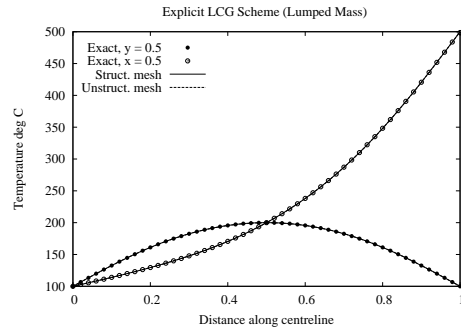
Fig. 11. 2D heat conduction problem using Mesh A.

Implicit LCG methods were the fastest, giving steady state results in under a second for Mesh A. The lumped mass version of the explicit global Galerkin was relatively faster than the explicit LCG method with lumped mass. This is expected as the LCG method needs an extra flux calculation step.

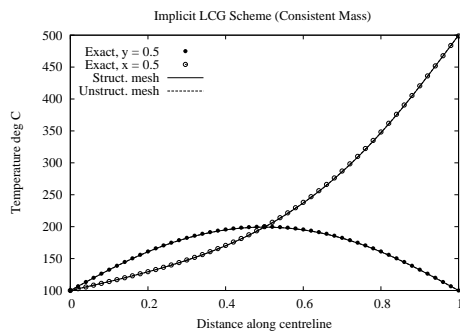
The convergence histories to steady state for all six variations are shown in Figure 13(a) and 13(b). During the computations it was found that the explicit LCG method with lumped mass allowed a slightly larger value of time-step than its global Galerkin counterpart. This can be seen in both graphs as the explicit LCG method converges at a faster rate than global Galerkin method. The convergence rates of the lumped mass and consistent mass implicit LCG methods are similar and much faster than explicit methods.



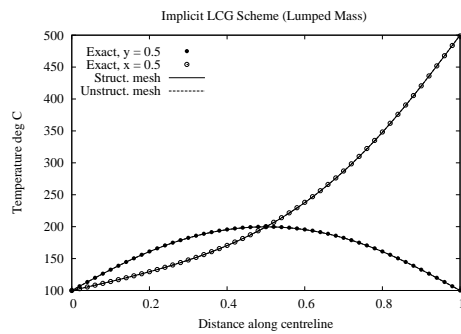
(a) Explicit LCG (consistent mass)



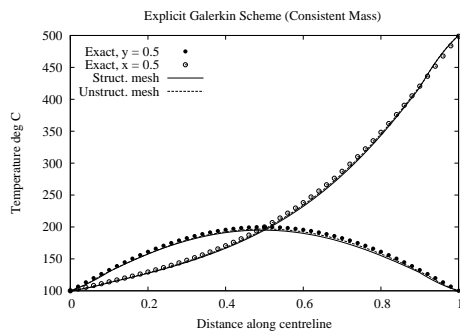
(b) Explicit LCG (lumped mass)



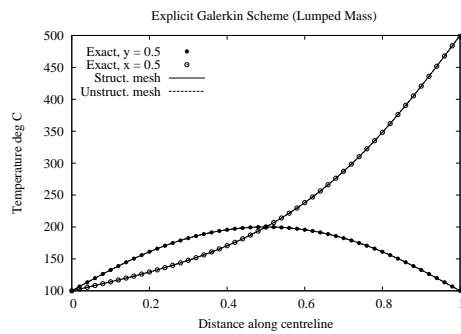
(c) Implicit LCG (consistent mass)



(d) Implicit LCG (lumped mass)



(e) Explicit global Galerkin (consistent mass)

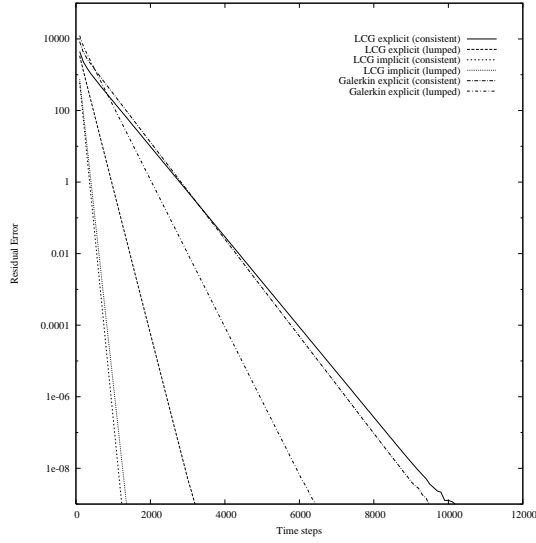


(f) Explicit global Galerkin (lumped mass)

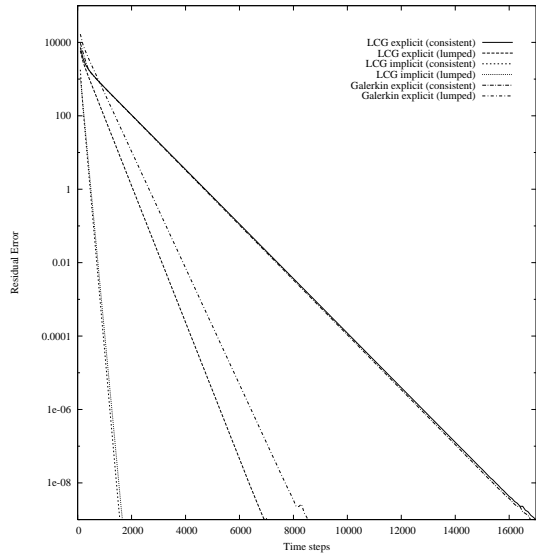
Fig. 12. 2D Heat Conduction, Comparison of Temperature along centre-lines with exact solution

6.3 Convection-Diffusion Problems

The first convection-diffusion problem re-examined here is the pure convection problem with a jump. Again the computational domain is a unit square and



(a) Mesh A



(b) Mesh C

Fig. 13. Convergence history to steady state

the flow is two-dimensional in nature with a constant velocity. The direction of which is skewed at an angle θ to the x_1 axis. It is used here to further demonstrate that LCG method can be readily used with established stabilized methods without any detrimental effect on the solution. The inlet boundary data presents a discontinuity in the scalar variable, and natural downwind boundary conditions are placed at the outlet. At the bottom side and small bottom portion of left vertical side, the variable is equal to zero. The rest of the left vertical side is subjected to $\phi = 1$. We consider solutions to this

Table 1
Total CPU times

Method	Mesh A	Mesh C
Explicit LCG (consistent mass)	5.75s	12.77s
Explicit LCG (lumped mass)	1.70s	4.81s
Implicit LCG (consistent mass)	0.78s	1.22s
Implicit LCG (lumped mass)	0.81s	1.28s
Explicit global Galerkin (consistent mass)	51.20s	154.67s
Explicit global Galerkin (lumped mass)	1.30s	1.91s

problem at angles $\theta = 30^\circ$ and 45° with $k = 1 \times 10^{-4}$ and $|U| = 1$, on both structured and unstructured meshes.

For this problem, CG method is used on meshes B and D. The problem is also solved using SUPG stabilization, but the contours produced are similar, and thus the results are not presented here.

The results for structured, Mesh B, are given in Figure 14. At $\theta = 45^\circ$, the quality of all six versions are high and differ little from each other. This is primarily due to mesh orientation along the discontinuity. At $\theta = 30^\circ$, however, the convected discontinuity travels through elements and the computed contours at this skew angle are not as sharp as the solutions computed at $\theta = 45^\circ$. At $\theta = 30^\circ$, the consistent mass implicit LCG method gave the most diffused solution. The other five versions give better quality solutions and are in close agreement with each other. The solutions obtained on Mesh D are given in Figure 15. All six methods give similar results for both $\theta = 30^\circ$ and $\theta = 45^\circ$. Generally the results on this mesh are more diffused, but considering the unstructured nature of the mesh, good non-oscillatory results are obtained.

6.4 Mesh Convergence Properties of the LCG Method

The order of grid convergence describes the behavior of the solution error E as a function of mesh element size h , i.e.,[33]

$$E = \tilde{\phi} - \phi = Ch^q + H.O.T. \quad (30)$$

A convergence study was performed in this paper to compute the L_2 error for various Péclet numbers using CG method. Structured Meshes A and B we

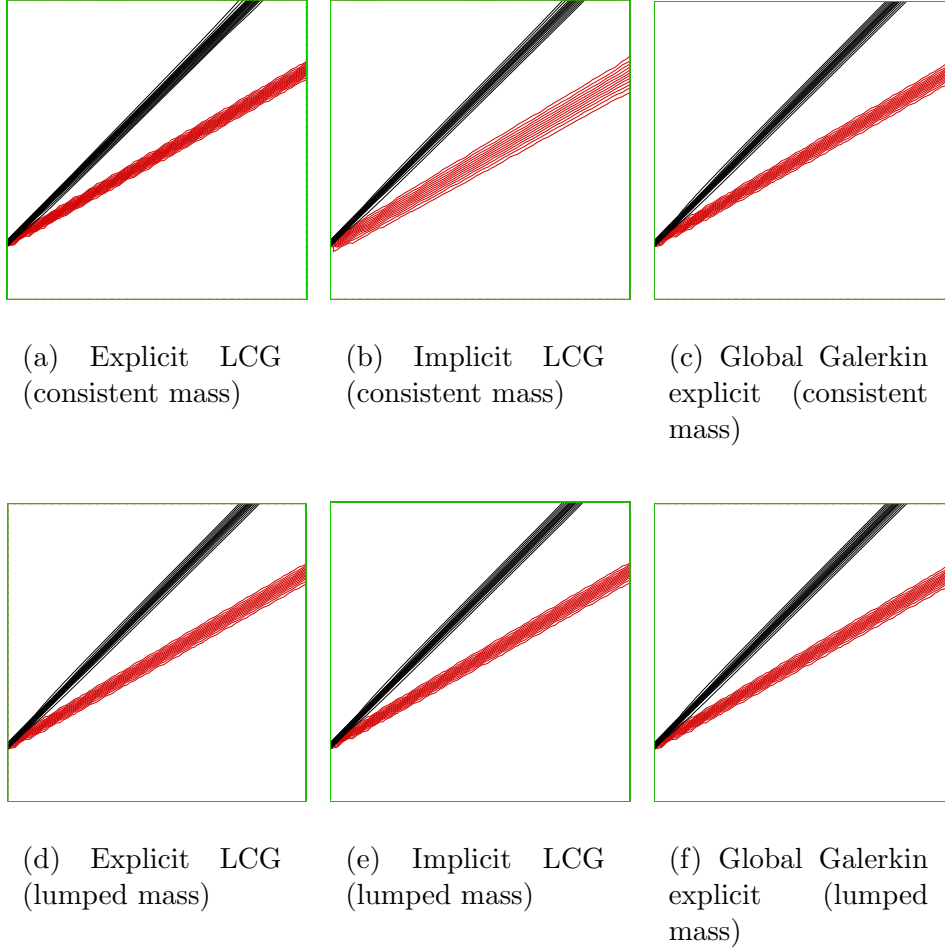


Fig. 14. Characteristic Galerkin stabilized steady-state solutions using Mesh C for the 2D convection of discontinuous inlet ($\theta = 30^\circ, 45^\circ$).

used in this study along with other structured meshes of varying element size. The problem is again a convection-diffusion problem. However, the difference here is that a source term of the form

$$Q(x_1) = 4u_1x_1^3 - 12kx_1^2 \quad (31)$$

is added to the RHS of the governing equation. At left boundary $\phi = 0$ and at the right boundary $\phi = 1$ are imposed. The top and bottom boundaries are assumed have zero flux conditions. This problem has an exact solution of

$$\phi(x_1) = x_1^4 \quad (32)$$

The source term is, for the LCG methods, applied to the RHS forcing vector of the elemental equation sets. The error E along the mid-horizontal line is

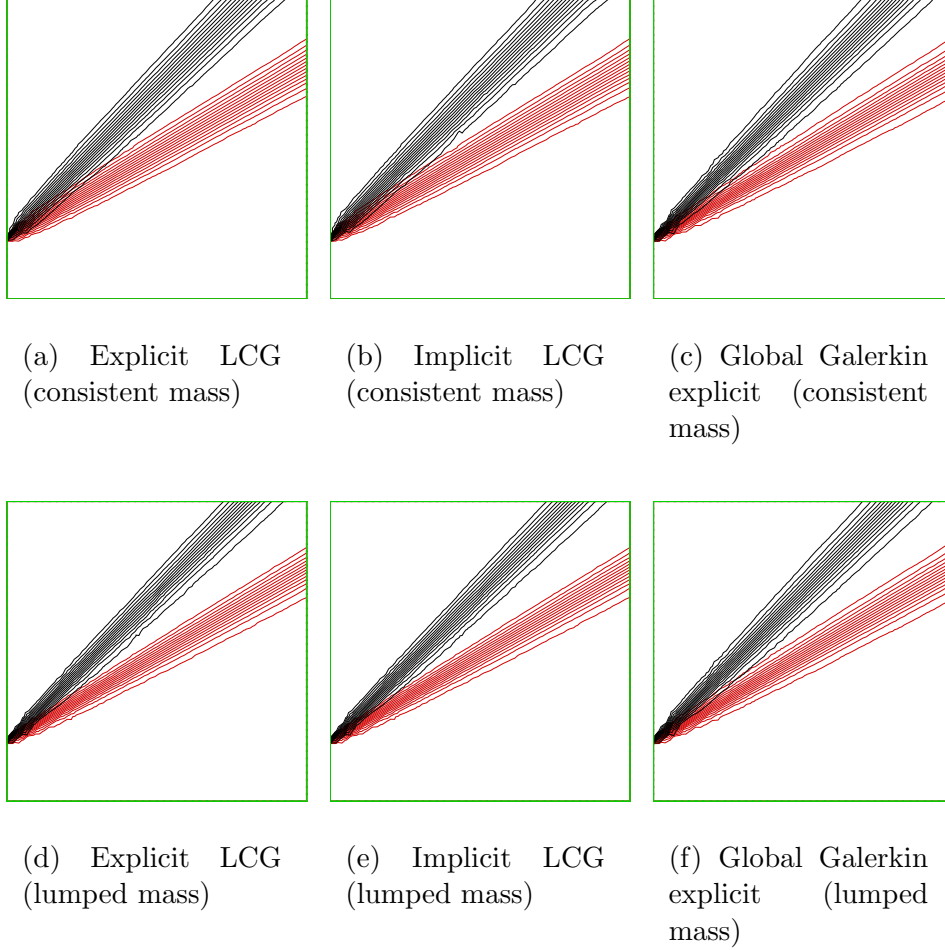


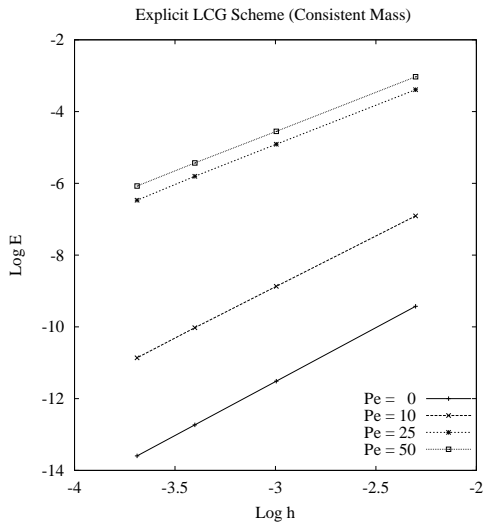
Fig. 15. Characteristic Galerkin stabilized steady-state solutions using Mesh D for the 2D convection of discontinuous inlet ($\theta = 30^\circ, 45^\circ$).

calculated using

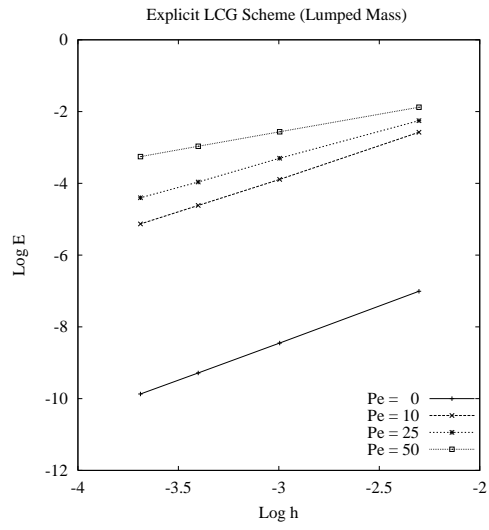
$$E^2 = \int_{x_1=0}^L (\tilde{\phi} - \phi)^2 dx_1 \quad (33)$$

Only the velocity in the x_1 direction is varied to obtain the desired Péclet number. A k value equal to unity and $u_2 = 0$ are used.

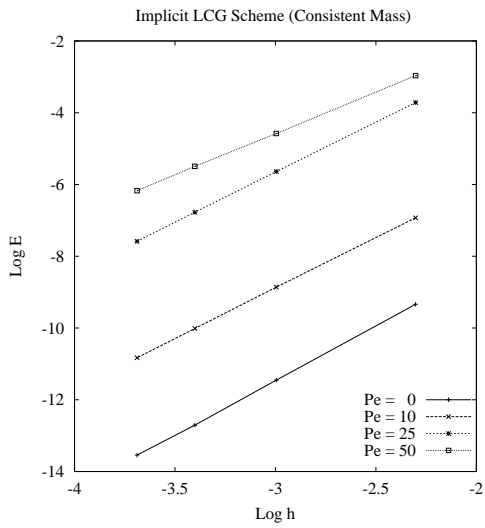
Figure 16 shows the convergence rates for different values of Péclet number. The convergence rates are also listed in Table 2. As seen consistent mass versions of the LCG method produces a third order convergence for the purely diffusive problem. This is consistent with the rate obtained by Donea et al. [34] for quadratic elements using the global Galerkin method. As the Péclet number increases, the convergence rate decreases. At $Pe = 50$ the convergence rates for the consistent mass LCG methods are over two. It was also found



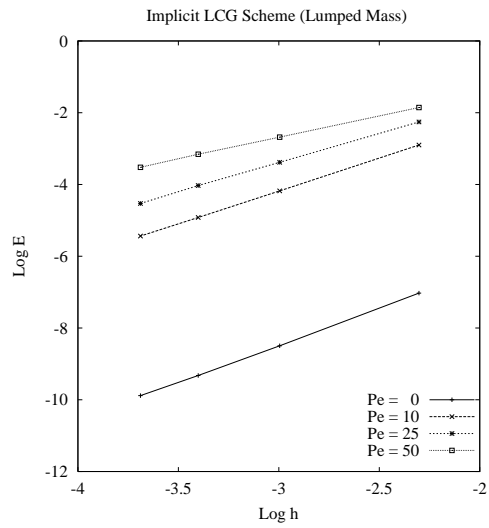
(a) LCG explicit (consistent mass)



(b) LCG explicit (lumped mass)



(c) LCG implicit (consistent mass)



(d) LCG implicit (lumped mass)

Fig. 16. L_2 Rates of Mesh Convergence using Quadratic Elements

that lumping the quadratic element mass matrix, for both the explicit and the implicit LCG schemes, had an adverse effect on the mesh convergence rate giving second order accuracy for diffusion and much smaller rates for convection dominated problems.

Table 2

Calculated L_2 rates of mesh convergence for $Pe = 0$ and $Pe = 50$, using quadratic-triangle elements

Method	$Pe = 0$	$Pe = 10$	$Pe = 25$	$Pe = 50$
Explicit LCG (consistent mass)	3.02	2.85	2.22	2.20
Explicit LCG (lumped mass)	2.09	1.84	1.55	0.99
Implicit LCG (consistent mass)	3.03	2.81	2.79	2.31
Implicit LCG (lumped mass)	2.08	1.83	1.64	1.20
Donea et al. (SUPG) [34]	3.00	2.22	2.16	2.15

7 Acknowledgements

Authors acknowledge Professor K Morgan, School of Engineering, University of Wales Swansea, for his valuable comments on an earlier version of the paper.

8 Conclusions

The LCG method has been investigated using both explicit and implicit approaches. Its robustness has been illustrated on both linear and quadratic triangular elements. If the standard consistent way of imposing the edge fluxes is used, the LCG method is identical to the global Galerkin method except on global boundaries. However, the LCG method has the advantage of solving smaller equation sets and it provides explicit element wise conservation of fluxes. The consistent mass versions of the LCG method have superior mesh convergence rates compared to that of the other methods.

References

- [1] A. Mizukami, A mixed finite element method for boundary flux computation, *Computer Methods in Applied Mechanics and Engineering* **57**, 239, 1986.
- [2] T. J. R. Hughes, L. P. Franca, I. Harari, M. Mallet, F. Shakib, and T. E. Spelce, Finite Element Method for High-Speed Flows: Consistent Calculation of Boundary Flux. *Paper No. AIAA-87-0556, AIAA 25th Aerospace Sciences Meeting*, Reno, Nevada 1987.
- [3] P. M. Gresho, R. L. Lee, R. L. Sani, M. K. Maslanik, and B. E. Eaton, The consistent Galerkin FEM for computing derived boundary quantities in thermal

and/or fluids problems, *International Journal for Numerical Methods in Fluids*, **7**, 371, 1987.

- [4] M. Oshima, T. J. R. Hughes, and K. Jansen, Consistent finite element calculation of boundary and internal fluxes, *International Journal of Computational Fluid Dynamics*, **9**, 227, 1998.
- [5] T.R.J. Hughes, G. Engel, L. Mazzei and M.G. Larson, The continuous Galerkin method is locally conservative, *Journal of Computational Physics*, **163**, 467 - 488, 2000.
- [6] T.R.J. Hughes, G.N. Wells. Conservation properties for the Galerkin and stabilised forms of the advection-diffusion and incompressible Navier-Stokes equations. *Computer Methods in Applied Mechanics and Engineering*, **194**, 1141-1159, 2005.
- [7] W.H. Reed and T.R. Hill. Triangular mesh methods for the neutron transport equation. *Technical report LA-UR-73-479*, Los Alamos Scientific Laboratory, 1973.
- [8] On a Finite Element Method for Solving the Neutron Transport Equation. Etd. Carl de Boor, *Mathematical Aspects of Finite Elements in Partial Differential Equations*, Proceedings of a Symposium Conducted by the Mathematic Research Center, Uni. Wisconsin-Madison, April 1-3, 1974.
- [9] G.Chavent and G. Salzano, A Finite Element Method for the 1D water flooding problem with gravity, *Journal of Computational Physics*, **45**, 307, 1982.
- [10] G.Chavent and B. Cockburn, The local projection P^0P^1 - discontinuous Galerkin finite element method for scalar conservation laws. *RAIRO Modél. Math. Anal.Numer.*, 23:565-592, 1989
- [11] B. Cockburn and C-W. Shu, TVB Runge-Kutta local projection discontinuous Galerkin finite element method for scalar conservation laws II: General framework. *Math. Comp.*, 52:411-435, 1989
- [12] B. Cockburn, S.Y. Lin, and C-W. Shu, TVB Runge-Kutta local projection discontinuous Galerkin finite element method for conservation laws III: One Dimensional systems *Journal of Computational Physics* **84**,90-113, (1989)
- [13] B. Cockburn, S. Hou, and C-W. Shu, TVB Runge-Kutta local projection discontinuous Galerkin finite element method for conservation laws IV: The Multidimensional case *Math. Comp.*, 54:545-581, (1990)
- [14] B. Cockburn and C-W. Shu, The Runge-Kutta local projection P^1 discontinuous Galerkin finite element method for scalar conservation laws. *RAIRO Modél. Math. Anal.Numer.*, 25:337-361, 1991
- [15] B. Cockburn and C-W. Shu, The Runge-Kutta discontinuous Galerkin finite element method for conservation laws V: Multidimensional systems *Journal of Computational Physics* **141**,199-224, (1998)
- [16] B. Cockburn, Disconuous Galerkin Methods for Convection Dominated Problems. *High-Order Methods for Computational Science and Engineering*, Vol.9, Springer-Verlag, Berlin, 1999.

- [17] B. Cockburn, G.E. Karniadakis and C-W. Shu, (Eds.), The Development of Discontinuous Galerkin Methods. *Discontinuous Galerkin Method. Theory, Computation and Applications*, Lecture Notes in Computational Science and Engineering, 3-50, Springer, Berlin, 2000.
- [18] O.C. Zienkiewicz, R.L. Taylor, S.J. Sherwin and J. Peiro, On discontinuous Galerkin methods, *International Journal for Numerical Methods in Engineering*, **58**, 1119 - 1148, 2003.
- [19] B. Cockburn, G. Kanschat, D. Schötzau. The Local discontinuous Galerkin methods for linear incompressible flow: A review, Computer and Fluids (Special Issue: Residual based methods and discontinuous Galerkin schemes) *Computers and Fluids* **34** 2005 491-506.
- [20] T.J.R. Hughes, G. Scovazzi, P.B. Bochev and A. Buffa, A multiscale discontinuous Galerkin method with the computational structure of a continuous Galerkin method, *Computer Methods in Applied Mechanics and Engineering*, 195, 2761 - 2787, 2006.
- [21] P. Nithiarasu, A simple locally Conservative Galerkin (LCG) Finite Element Method for Transient Conservation Equations, *Numerical Heat Transfer, Part B Fundamentals*, **46**, 357 - 370, 2004.
- [22] O.C. Zienkiewicz, R.L. Taylor, and J. Zhu *The Finite Element Method, Volume 1 The basis*, Sixth Edition, Elsevier Butterworth-Heinemann, Oxford, 2005.
- [23] A. N. Brooks and T.R.J. Hughes, Streamline upwind/Petrov-Galerkin formulations for convection dominated flows with particular emphasis on the incompressible Navier-Stokes equations, *Computer Methods in Applied Mechanics and Engineering*, **32**(1-3), 199 - 259, 1982.
- [24] C. G. Thomas and P. Nithiarasu, Influences of element size and variable smoothing on inviscid compressible flow solution, *International Journal of Numerical Method for Heat and Fluid Flow*, **15**, 420-428, 2005.
- [25] J. Donea and A. Huerta, *Finite Element Methods for Flow Problems*, Wiley, Chichester, 2003.
- [26] O.C. Zienkiewicz, R.L. Taylor, and P. Nithiarasu *The Finite Element Method for Fluid Dynamics*, Sixth Edition, Elsevier Butterworth-Heinemann, Oxford, 2005.
- [27] R. Löhner, K. Morgan and O.C. Zienkiewicz, The solution of non-linear hyperbolic equation systems by the finite element method, *International Journal for Numerical Methods in Fluids*, **4**, 1043-1063, 1984.
- [28] O.C. Zienkiewicz and R. Codina, 'A general algorithm for compressible and incompressible flow. I. The split, characteristic-based scheme', *International Journal for Numerical Methods in Fluids*, 1995, **20**(8-9), 869-885.
- [29] P. Nithiarasu, R. Codina and O.C. Zienkiewicz, The Characteristic Based Split (CBS) Scheme - a unified approach to fluid dynamics. *International Journal for Numerical Methods in Engineering*, 66, 1514-1546, 2006.

- [30] P. Nithiarasu and O.C. Zienkiewicz, Analysis of an explicit and matrix free fractional step method for incompressible flows, *Computer Methods in Applied Mechanics and Engineering*, 195, 5537-5551, 2006.
- [31] J. Donea, B. Roig and A. Huerta, High-order accurate time-stepping schemes for convection-diffusion problems, *Computer Methods in Applied Mechanics and Engineering*, 182, 249-275, 2000.
- [32] J.P. Holman, *Heat Transfer*, McGraw Hill Publishers, Singapore, 1989.
- [33] J. Abanto, D Pelletier, A Gadon, J-Y Trepanier and M Reggio, Verification of some commercial CFD codes on atypical CFD problems, AIAA Paper 2005-0682, 10 - 13 January 2005, Reno.
- [34] J. Donea, T. Belytschko, and P. Smolinski, A generalized Galerkin method for steady convection-diffusion problems with application to quadratic shape functions, *Comp. Meth. Appl. Mech. Eng.*, , **48**, 25-43, 1985.